

A NONLINEAR VISION BASED TRACKING SYSTEM FOR COORDINATED CONTROL OF MARINE VEHICLES

P. Oliveira*, A. Pascoal*, I. Kaminer[†]

* Institute for Systems and Robotics (ISR) and
Department of Electrical Engineering, Instituto Superior Técnico (IST),
Av. Rovisco Pais, 1049-001 Lisboa, Portugal
fax: +351 21 8418291
e-mail: {pjcro, antonio}@isr.ist.utl.pt
<http://dsor.isr.ist.utl.pt/>

[†] Department of Aeronautics and Astronautics,
Naval Postgraduate School, Monterey, CA 93943, USA
e-mail: kaminer@aa.nps.edu.mil

Keywords: Nonlinear Filters, LPVs, Autonomous Vehicles, Vision Systems.

Abstract

This paper proposes a vision based tracking system to estimate the position and velocity of an Autonomous Underwater Vehicle (AUV) relative to an Autonomous Surface Craft (ASC). Nonlinear estimator design builds on the theory of linear parametrically varying (LPV) systems. The theoretical framework adopted provides a powerful tool for regional estimator stability and performance analysis. Simulations illustrate the performance of the tracker developed.

1 Introduction

In recent years there has been increasing interest in the use of fleets of autonomous vehicles to perform complex missions in air, on land, and at sea. See (IEEE, 2000) and the references therein for illustrative examples. See also (Pascoal *et al.*, 2000; ASIMOV, 1998-1999) for an example of cooperative motion control of the Delfim Autonomous Surface Craft (ASC) and the Infante Autonomous Underwater Vehicle (AUV) in the marine robotics area.

In the latter application, data exchange between the two vehicles must rely on acoustic communications due to the strong attenuation experienced by electromagnetic waves in the water. Furthermore, in order to meet stringent bandwidth requirements imposed by the need to transmit video/acoustic sensor data, communications are essentially restricted to the vertical channel so as to avoid multipath effects. Meeting these objectives requires the design and development of navigation, guidance, and control algorithms with reduced sensor data exchange between the two vehicles.

These requirements led naturally to the problem of implementing a tracker on board the ASC to provide estimates of the relative position and velocity of both platforms. Standard solutions rely on the use of Ultra-Short Baseline positioning systems (USBL) or, more recently, on the GPS Intelligent Buoy tracker system (GIB) (Instrumentation, 1999). However, their high cost, complex installation, and precise calibrating requirements motivated the need to pursue alternative solutions to avoid the use of cumbersome acoustic positioning systems. The paper proposes a structure for a tracker that complements data from a camera with that available from other conventional motion sensors. This solution is plu-

sible in shallow water and under high visibility conditions, when an artificial feature associated with the AUV can be extracted from images obtained on board the ASC.

Position, velocity, and attitude estimates for the ASC are provided by a navigation system installed on board the vehicle (Oliveira, 2001) based on measurements from a Differential GPS, a Doppler sonar log, and an Attitude and Heading Reference System (AHRS). The installation of a calibrated video camera on the ASC is required to provide access to the coordinates of an artificial feature of the AUV in the image, such as a strobe light. To solve the ambiguity associated with the image sensor that maps the 3D world into 2D image coordinates, an additional measurement related to the AUV position is required. Alternative measurements such as AUV depth or the distance between the two vehicles can be provided by a depth cell or by an acoustic ranging sensor, respectively. Due to space limitations, only the first situation is studied here. In this case, only data on the deviations from the nominal depth envelope are required to be transmitted through the acoustic communication link.

The key contribution of this paper is the development of a vision based nonlinear tracker that departs considerably from classical solutions. The methodology adopted for system design builds on the theory of Linear Parametrically Varying (LPV) Systems (Scherer, 2000), which is shown to provide a new powerful framework for the design of navigation filters for autonomous vehicles that rely on inertial and vision sensors. The new methodology leads to filter structures that are intuitively appealing. Furthermore, it provides tools to assess regional (non-local) stability and performance.

The paper is organized as follows. Section 2 reviews some background material on linear time-varying systems, induced operator norms, and linear parametrically varying (LPV) systems. In Section 3, some notation and the basic kinematic relations for the autonomous vehicles present in the mission scenarios envisioned are described. The sensor suite to be installed on board the vehi-

cles is discussed and the resulting nonlinear synthesis model that will be used for tracker design are also introduced. Section 4 presents the main results of the paper by providing a solution to the tracking problem considered. Section 5 discusses simulation results. Finally, Section 6 contains the conclusions and discusses issues that warrant further research.

2 Mathematical background

This section introduces some technical results for the study of linear parametrically varying (LPV) systems. The notation and basic theory are by now standard, see (Becker and Packard, 1994), (Boyd *et al.*, 1994), (Scherer, 2000) and (Vidyasagar, 1985). In what follows we assume the reader is familiar with the notions of L_2 and L_∞ spaces of functions.

Let \mathcal{Q} (a compact subset of \mathcal{R}^p) denote a parameter variation set and let \mathcal{F}_ρ be the set of all continuous functions mapping \mathcal{R}^+ to \mathcal{Q} . We will restrict ourselves to the class of LPV systems $\mathcal{G}_{\mathcal{F}_\rho}$ with finite-dimensional state-space realizations

$$\Sigma_{\mathcal{G}_{\mathcal{F}_\rho}} = \begin{cases} \dot{\mathbf{x}}(t) &= A(\rho(t))\mathbf{x}(t) + B(\rho(t))\mathbf{w}(t), \\ \mathbf{z}(t) &= C(\rho(t))\mathbf{x}(t) \end{cases} \quad (1)$$

where $\rho \in \mathcal{F}_\rho$, $\mathbf{x}(t) \in \mathbb{R}^n$ is the state, $\mathbf{w}(t) \in \mathbb{R}^m$ is the input, and $\mathbf{z}(t) \in \mathbb{R}^p$ is the system output. The symbols $A(\rho(t))$, $B(\rho(t))$, and $C(\rho(t))$ denote matrices of bounded, piece-wise continuous functions of time, depending on a continuous time-varying parameter $\rho(t)$ of proper dimensions. In an LPV system the parameter $\rho \in \mathcal{F}_\rho$ is assumed to be unknown but measurable online. Note that the symbol $\mathcal{G}_{\mathcal{F}_\rho}$ denotes both an LPV system and its particular realization $\Sigma_{\mathcal{G}_{\mathcal{F}_\rho}}$, as the meaning will be clear from the context.

An LPV system $\mathcal{G}_{\mathcal{F}_\rho}$ is said to be stable if its \mathcal{L}_2 induced operator norm

$$\begin{aligned} \|\mathcal{G}_{\mathcal{F}_\rho}\|_{2,i} &= \sup_{\rho \in \mathcal{Q}} \|\mathcal{G}_\rho\|_{2,i} = \\ &= \sup_{\rho \in \mathcal{Q}} \sup\left\{ \frac{\|\mathcal{G}_\rho \mathbf{w}\|_2}{\|\mathbf{w}\|_2} : \mathbf{w} \in L_2, \|\mathbf{w}\|_2 \neq 0 \right\} \end{aligned} \quad (2)$$

is well defined and finite. The following result is instrumental in computing the \mathcal{L}_2 induced operator norm of a system.

Theorem 2.1 (Becker and Packard, 1994) Consider the LPV system $\mathcal{G}_{\mathcal{F}_\rho}$ with realization (1). Suppose there exists a positive definite, symmetric matrix $X \in \mathbb{R}^{n \times n}$ such that for all $\rho \in \mathcal{Q}$ the matrix inequality

$$A^T(\rho(t))X + XB(\rho(t))B^T(\rho(t))X + XA(\rho(t))\frac{C(\rho(t))C^T(\rho(t))}{\gamma^2} < 0. \quad (3)$$

holds. Then, for $x(0) = 0$, $\mathbf{w} \in L_2$, $\|\mathbf{w}\|_2 < 1$ and $\forall \rho \in \mathcal{Q}$

$$\lim_{t \rightarrow \infty} x(t) = 0$$

and $\|\mathcal{G}_{\mathcal{F}_\rho}\|_{2,i} < \gamma$.

The extension of these definitions to the case where the operator inputs \mathbf{w} and outputs \mathbf{z} belong to the space of essentially bounded functions of time is immediate (see (Vidyasagar, 1985)).

A system $\mathcal{G}_{\mathcal{F}_\rho}$ described by equation (2) is said to be finite-gain stable if its $\|\mathcal{G}_{\mathcal{F}_\rho}\|_{2,\infty}$ induced norm

$$\begin{aligned} \|\mathcal{G}_{\mathcal{F}_\rho}\|_{2,\infty} &= \sup_{\rho \in \mathcal{Q}} \|\mathcal{G}_\rho\|_{2,\infty} = \\ &= \sup_{\rho \in \mathcal{Q}} \sup\left\{ \frac{\|\mathcal{G}_\rho \mathbf{w}\|_\infty}{\|\mathbf{w}\|_2} : \mathbf{w} \in L_2, \|\mathbf{w}\|_2 \neq 0 \right\}, \end{aligned}$$

also referred to as the generalized \mathcal{H}_2 norm, is well defined and finite. See (Scherer, 2000) for the computation of $\|\mathcal{G}_{\mathcal{F}_\rho}\|_{2,\infty}$ by resorting to linear matrix inequalities.

Equipped with this set of results the AUV/ASC tracking problem will be formulated and a solution proposed and analyzed.

3 The tracker problem. Notation and design model

This section describes the tracker problem which is the main focus of this paper. For the sake of clarity, we first introduce some basic notation and summarize the kinematic relations. Next, the sensor suite that is used in the envisioned mission scenario is discussed and the corresponding measurements are related according to the kinematics of the problem at hand. Finally, the underlying nonlinear tracker synthesis model is presented.

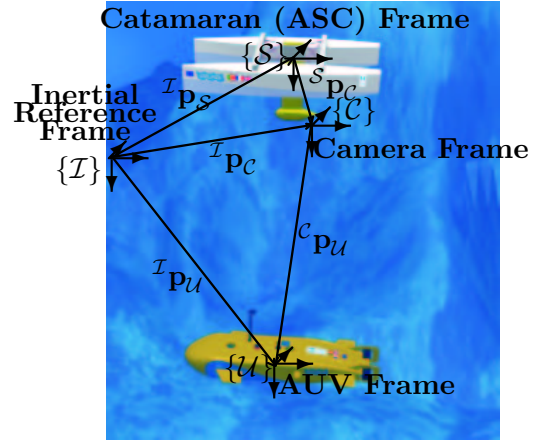


Figure 1: Reference frames and notation.

3.1 Notation

Let $\{\mathcal{I}\}$ be a fixed reference frame located at a given mission scenario origin, at mean sea level, and let $\{\mathcal{S}\}$ and $\{\mathcal{U}\}$ denote body-fixed frames that move with the ASC and the AUV, respectively, as depicted in figure 1. The following notation is required:

${}^{\mathcal{I}}\mathbf{p}_S$ - position of the origin of $\{\mathcal{S}\}$ in $\{\mathcal{I}\}$;

${}^{\mathcal{I}}\mathbf{p}_U$ - position of the origin of $\{\mathcal{U}\}$ in $\{\mathcal{I}\}$;

\mathbf{p} - position of the origin of $\{\mathcal{U}\}$ relative to $\{\mathcal{S}\}$, expressed in $\{\mathcal{I}\}$, i.e., $\mathbf{p} = {}^{\mathcal{I}}\mathbf{p}_U - {}^{\mathcal{I}}\mathbf{p}_S$;

${}^{\mathcal{I}}\mathbf{v}_S$ - linear velocity of the origin of $\{\mathcal{S}\}$ in $\{\mathcal{I}\}$;

${}^{\mathcal{I}}\mathbf{v}_U$ - linear velocity of the origin of $\{\mathcal{U}\}$ in $\{\mathcal{I}\}$;

$\boldsymbol{\lambda} := [\phi \ \theta \ \psi]^T$ - vector of roll, pitch, and yaw angles that parameterize locally the orientation of frame $\{\mathcal{S}\}$ with respect to $\{\mathcal{I}\}$;

$\boldsymbol{\omega} := [p \ q \ r]^T$ - angular velocity of $\{\mathcal{S}\}$ with respect to $\{\mathcal{I}\}$, resolved in $\{\mathcal{S}\}$;

3.2 Vehicles kinematics and the sensor suite

Given two frames $\{\mathcal{A}\}$ and $\{\mathcal{B}\}$, ${}^{\mathcal{A}}\mathcal{R}$ denotes the rotation matrix from $\{\mathcal{B}\}$ to $\{\mathcal{A}\}$. In particular, ${}^{\mathcal{I}}\mathcal{R}(\boldsymbol{\lambda})$ is the rotation matrix from $\{\mathcal{S}\}$ to $\{\mathcal{I}\}$,

parameterized locally by $\boldsymbol{\lambda}$. Since \mathcal{R} is a rotation matrix, it satisfies the orthogonality condition $\mathcal{R}^T = \mathcal{R}^{-1}$ that is, $\mathcal{R}^T \mathcal{R} = I$. Given the angular velocity vector $\boldsymbol{\omega}$, then

$$\dot{\boldsymbol{\lambda}} = Q(\boldsymbol{\lambda})\boldsymbol{\omega},$$

where $Q(\boldsymbol{\lambda})$ is a matrix that relates the derivative of $\boldsymbol{\lambda}$ with $\boldsymbol{\omega}$. It is well known (Britting, 1971) that

$$\frac{d}{dt} {}^{\mathcal{I}}\mathbf{p}_{\mathcal{S}} = {}^{\mathcal{I}}\mathbf{v}_{\mathcal{S}} = {}^{\mathcal{I}}_{\mathcal{S}}\mathcal{R}(\boldsymbol{\lambda}) {}^{\mathcal{S}}({}^{\mathcal{I}}\mathbf{v}_{\mathcal{S}}) \quad (4)$$

$$\frac{d}{dt} {}^{\mathcal{I}}_{\mathcal{S}}\mathcal{R}(\boldsymbol{\lambda}) = {}^{\mathcal{I}}_{\mathcal{S}}\mathcal{R}(\boldsymbol{\lambda}) \mathcal{S}(\boldsymbol{\omega}), \quad (5)$$

where ${}^{\mathcal{S}}({}^{\mathcal{I}}\mathbf{v}_{\mathcal{S}})$ is the ASC velocity relative to the inertial frame, expressed in \mathcal{S} (i.e., body fixed velocity) and

$$\mathcal{S}(\boldsymbol{\omega}) := \begin{bmatrix} 0 & -\omega_z & \omega_y \\ \omega_z & 0 & -\omega_x \\ -\omega_y & \omega_x & 0 \end{bmatrix} \quad (6)$$

is a skew symmetric matrix, that is, $\mathcal{S}^T = -\mathcal{S}$. The matrix \mathcal{S} satisfies the relationship $\mathcal{S}(a)b = a \times b$, where a and b are arbitrary vectors and \times denotes the cross product operation. Furthermore, $\|\mathcal{S}(\boldsymbol{\omega})\| = \|\boldsymbol{\omega}\|$.

The ASC is equipped with a set of sensors and its own navigation system, as described in (ASIMOV, 1998-1999). The navigation system provides estimates ${}^{\mathcal{I}}\mathbf{p}_{\mathcal{S}}$ and ${}^{\mathcal{I}}\mathbf{v}_{\mathcal{S}}$ of the position and velocity of the body fixed frame $\{\mathcal{S}\}$ relative to the inertial frame $\{\mathcal{I}\}$, respectively. Estimates of the attitude $\boldsymbol{\lambda}$ are also available and, as a consequence, ${}^{\mathcal{I}}_{\mathcal{S}}\mathcal{R}(\boldsymbol{\lambda})$ is known.

The tracker design problem at hand will be cast in the framework of complementary filtering theory (see (Oliveira, 2001)). We now discuss the sensors used and the type of sensor data available. A video camera pointing down, capable of detecting an artificial feature of the AUV (such as a strobe light), is installed on board the ASC. Simple geometric considerations show that the camera position ${}^{\mathcal{I}}\mathbf{p}_{\mathcal{C}}$ and its orientation ${}^{\mathcal{I}}_{\mathcal{C}}\mathcal{R}$ are given by (see figure 1)

$${}^{\mathcal{I}}\mathbf{p}_{\mathcal{C}} = {}^{\mathcal{I}}\mathbf{p}_{\mathcal{S}} + {}^{\mathcal{I}}_{\mathcal{S}}\mathcal{R}(\boldsymbol{\lambda}) {}^{\mathcal{S}}\mathbf{p}_{\mathcal{C}} \quad (7)$$

and

$${}^{\mathcal{I}}_{\mathcal{C}}\mathcal{R}(\boldsymbol{\lambda}) = {}^{\mathcal{I}}_{\mathcal{S}}\mathcal{R}(\boldsymbol{\lambda}) {}^{\mathcal{S}}_{\mathcal{C}}\mathcal{R},$$

respectively. Assume without loss of generality that ${}^{\mathcal{C}}_{\mathcal{S}}\mathcal{R} = I$ and ${}^{\mathcal{S}}\mathbf{p}_{\mathcal{C}} = 0$, that is, $\{\mathcal{C}\} = \{\mathcal{S}\}$. Then, ${}^{\mathcal{I}}\mathbf{p}_{\mathcal{C}} = {}^{\mathcal{I}}\mathbf{p}_{\mathcal{S}}$ and ${}^{\mathcal{I}}_{\mathcal{C}}\mathcal{R} = {}^{\mathcal{I}}_{\mathcal{S}}\mathcal{R}$. Similarly,

$${}^{\mathcal{I}}\mathbf{p}_{\mathcal{U}} = {}^{\mathcal{I}}\mathbf{p}_{\mathcal{C}} + {}^{\mathcal{I}}_{\mathcal{C}}\mathcal{R}(\boldsymbol{\lambda}) {}^{\mathcal{C}}\mathbf{p}_{\mathcal{U}}. \quad (8)$$

Using relations (7) and (8), the position of the origin of $\{\mathcal{U}\}$ relative to $\{\mathcal{C}\}$, expressed in $\{\mathcal{C}\}$, yields

$${}^{\mathcal{C}}\mathbf{p} = {}^{\mathcal{C}}_{\mathcal{I}}\mathcal{R}({}^{\mathcal{I}}_{\mathcal{C}}\mathcal{R}(\boldsymbol{\lambda}) ({}^{\mathcal{I}}\mathbf{p}_{\mathcal{U}} - {}^{\mathcal{I}}\mathbf{p}_{\mathcal{S}})) \quad (9)$$

which can be written in compact form as ${}^{\mathcal{C}}\mathbf{p} = \frac{\mathcal{C}}{\mathcal{I}}\mathcal{R}(\boldsymbol{\lambda})\mathbf{p}$. Suppose an artificial feature is placed at the origin of $\{\mathcal{U}\}$. Processing of the video images acquired with the camera installed on board the ASC allows for the feature extraction of its 2D coordinates

$$\begin{bmatrix} u_c \\ v_c \end{bmatrix} = \begin{bmatrix} f x_c / z_c \\ f y_c / z_c \end{bmatrix} \quad (10)$$

in the image plane, where f denotes the focal distance for the pinhole model of the imaging system. This key relation in computer vision (Horn, 1985) is a nonlinear mapping from \mathcal{R}^3 to \mathcal{R}^2 , leading to an ambiguity in the coordinate measurements in the image plane. To solve this ambiguity, an additional measurement related to the AUV position is required, such as its depth or the distance between the AUV and the ASC. In what follows we assume a depth cell is used. Assuming the ASC is at depth zero, the relative z coordinate (which equals the AUV depth) is obtained from the third row of equation (9) as

$$z = -s(\theta)x_c + c(\theta)s(\phi)y_c + c(\theta)c(\phi)z_c, \quad (11)$$

where $s(\cdot)$ and $c(\cdot)$ are the trigonometric sinus and co-sinus functions, respectively. This relation assumes that wave effects can be easily accounted for, due to the existence of a navigation system on board the ASC.

In order to implement the desired estimator structure, the complementary measurement of the AUV velocity relative to the ASC is required.

A sensor that would measure this relative velocity, based on the Doppler effect experienced by acoustic waves travelling between the two vehicles, would be a possibility. However, this option requires sensors that are expensive or difficult to develop and will therefore not be used in the proposed framework. Instead, an approximate relation that is introduced next will be exploited along this work. The relationship builds on the assumption that the AUV travels at constant velocity.

From (9),

$${}^{\mathcal{I}}\mathbf{p}_u = {}^{\mathcal{I}}\mathbf{p}_s + {}^{\mathcal{I}}\mathcal{R}(\boldsymbol{\lambda}) {}^c\mathbf{p}.$$

The velocities of the ASC and the AUV can be related as

$${}^{\mathcal{I}}\mathbf{v}_u = {}^{\mathcal{I}}\mathbf{v}_s + \frac{d}{dt}({}^{\mathcal{I}}\mathcal{R} {}^c\mathbf{p}). \quad (12)$$

Assume for the time being that the the velocity of the AUV is zero (this restriction will be lifted shortly). Then,

$$\frac{d}{dt}({}^{\mathcal{I}}\mathcal{R} {}^c\mathbf{p}) = -{}^{\mathcal{I}}\mathbf{v}_s,$$

i.e., the velocity of the AUV as seen by the ASC and expressed in the inertial frame $\{\mathcal{I}\}$ is, apart from a change in signal, the same as the velocity of the ASC in $\{\mathcal{I}\}$. Assume a Doppler sonar log installed on board the ASC provides measurements ${}^S({}^{\mathcal{I}}\mathbf{v}_s)$ of the velocity of the ASC with respect to $\{\mathcal{U}\}$, expressed in $\{\mathcal{S}\}$. Then, (4) can be rewritten to yield

$$\frac{d}{dt}({}^{\mathcal{I}}\mathcal{R} {}^c\mathbf{p}) = -{}^{\mathcal{I}}\mathcal{R}(\boldsymbol{\lambda}) {}^S({}^{\mathcal{I}}\mathbf{v}_s).$$

The assumption above motivates the use of an estimator with a bank of integrators aimed at estimating biases in the inertial velocity measurements. The estimated biases corresponds to the deviation in the estimated ASC velocity due to the actual AUV velocity, which is different from zero.

3.3 Design model

In the following, the underlying design model that plays a central role in the design of the tracker is

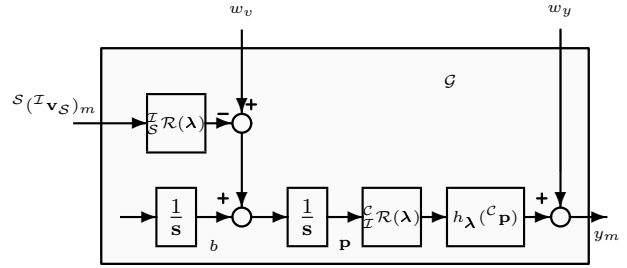


Figure 2: Estimator model.

presented. The model is based on the kinematic relations presented above. The resulting system \mathcal{G} has the realization

$$\Sigma_{\mathcal{G}} = \begin{cases} \dot{\mathbf{p}} &= -{}^{\mathcal{I}}\mathcal{R}(\boldsymbol{\lambda}) {}^S({}^{\mathcal{I}}\mathbf{v}_s)_m + b + w_v \\ \dot{b} &= 0 \\ y_m &= h_{\boldsymbol{\lambda}}({}^c\mathbf{p}) + w_y, \end{cases} \quad (13)$$

where y_m contains the measurement of $y = [u_c \ v_c \ z]^T$ and $h_{\boldsymbol{\lambda}}({}^c\mathbf{p}) : \mathcal{R}^3 \rightarrow \mathcal{R}^3$ is obtained by putting together relations (10) and (11) for the camera model and depth measurement, respectively. Vector b denotes velocity bias that must be estimated. The velocity of the ASC is considered as an input to the model, as depicted in figure 2.

4 Tracker design and analysis

The problem at hand can be described as that of determining estimates of the relative position and velocity of the AUV with respect to the ASC, based on the sensor package described before. The filter design model is the one in figure 2. In this section, a structure for a nonlinear estimator is proposed and analyzed.

Consider that the orientation of the camera frame installed on board the ASC is constrained to be in the compact set given by

$$\Lambda_c = \{\boldsymbol{\lambda} : |\phi| \leq \phi_{max}, |\theta| \leq \theta_{max}\}, \quad (14)$$

and that the relative position of the AUV relative to the ASC, expressed in $\{\mathcal{C}\}$, is constrained to

be in

$$\mathcal{P}_c = \left\{ \begin{array}{l} {}^c\mathbf{p} = [x_c \ y_c \ z_c]^T \quad : \quad \begin{array}{l} \underline{x} \leq x_c \leq \bar{x}, \\ \underline{y} \leq y_c \leq \bar{y}, \\ 0 < \underline{z} \leq z_c \leq \bar{z} \end{array} \end{array} \right\} \quad (15)$$

Notice that the yaw angle ψ is not constrained, $\underline{x} \dots \bar{z}$ can be chosen according to the mission scenario and the expected vehicles dynamics, and z_c is positive given the fact that we are dealing with an underwater vehicle and the inertial frame origin $\{\mathcal{I}\}$ is located at mean sea level. Let the estimates of the relative position ${}^c\mathbf{p}$ and velocity ${}^c\mathbf{v}$ be written as $\hat{\mathbf{p}}_c$ and $\hat{\mathbf{v}}_c$, respectively. It will be required that the relative position estimate ${}^c\hat{\mathbf{p}}$ lie in the compact set

$$\hat{\mathcal{P}}_c = \left\{ \begin{array}{l} {}^c\hat{\mathbf{p}} : \begin{array}{l} |\hat{x}_c - x_c| \leq \bar{x} - \underline{x} + dx, \\ |\hat{y}_c - y_c| \leq \bar{y} - \underline{y} + dy, \\ |\hat{z}_c - z_c| \leq \bar{z} - \underline{z} + dz \end{array} \end{array} \right\}, \quad (16)$$

where dx , dy , and dz are positive numbers and $dz < \underline{z}$.

The estimator structure proposed in this paper builds on a key result that was introduced in (Rizzi and Koditscheck, 1996). See also (Kaminer *et al.*, 2001), where the same structure is used in a navigation system for automatic landing of autonomous aircraft. This algebraic result, which relates errors in the image plane with errors observed in the inertial frame, is stated in the following lemma:

Lemma 4.1 *Let $h_{\boldsymbol{\lambda}}(\dots)$ be the mapping function introduced in section 3. Then*

$$h_{\boldsymbol{\lambda}}({}^c\hat{\mathbf{p}}) - h_{\boldsymbol{\lambda}}({}^c\mathbf{p}) = L({}^c\hat{\mathbf{p}}, {}^c\mathbf{p})H({}^c\hat{\mathbf{p}})({}^c\hat{\mathbf{p}} - {}^c\mathbf{p}), \quad (17)$$

where

$$L({}^c\hat{\mathbf{p}}, {}^c\mathbf{p}) = \begin{bmatrix} \hat{z}_c/z_c & 0 & 0 \\ 0 & \hat{z}_c/z_c & 0 \\ 0 & 0 & 1 \end{bmatrix},$$

and $H({}^c\hat{\mathbf{p}})$ denotes the Jacobian of $h_{\boldsymbol{\lambda}}({}^c\hat{\mathbf{p}})$ with respect to ${}^c\hat{\mathbf{p}}$.

According to the definition of $h_{\boldsymbol{\lambda}}({}^c\hat{\mathbf{p}})$, the Jacobian is given by

$$H({}^c\hat{\mathbf{p}}) = \begin{bmatrix} f/\hat{z}_c & 0 & -f\hat{x}_c/\hat{z}_c^2 \\ 0 & f/\hat{z}_c & -f\hat{y}_c/\hat{z}_c^2 \\ -s(\theta) & c(\theta)s(\phi) & c(\theta)c(\phi) \end{bmatrix}$$

and verifies

$$|H({}^c\hat{\mathbf{p}})| = \frac{f}{\hat{z}_c^3} z_c.$$

Thus, it is invertible in the compact set of positions where the missions will take place. As a motivation to the structure of the estimator to be proposed, invert expression (17) to obtain

$${}^c\hat{\mathbf{p}} - {}^c\mathbf{p} = H^{-1}({}^c\hat{\mathbf{p}})L^{-1}({}^c\hat{\mathbf{p}}, {}^c\mathbf{p}) (h_{\boldsymbol{\lambda}}({}^c\hat{\mathbf{p}}) - h_{\boldsymbol{\lambda}}({}^c\mathbf{p})). \quad (18)$$

Assuming that $\hat{z}_c/z_c \approx 1$ yields $L({}^c\hat{\mathbf{p}}, {}^c\mathbf{p}) \approx I$, i.e.,

$$({}^c\hat{\mathbf{p}} - {}^c\mathbf{p}) = H({}^c\hat{\mathbf{p}})^{-1}(h_{\boldsymbol{\lambda}}({}^c\hat{\mathbf{p}}) - h_{\boldsymbol{\lambda}}({}^c\mathbf{p})). \quad (19)$$

The importance of this nonlinear relation is twofold: i) it can be used in the estimator as a way to relate errors in the sensor measurements with state variable errors, and ii) it holds the key to bring the estimator dynamics into the form of an LPV system.

4.1 Proposed solution

Motivated by the relation in (19), the solution proposed for the problem addressed in this paper is the tracker with realization

$$\Sigma_{\mathcal{T}} = \begin{cases} \dot{\hat{\mathbf{p}}} & = \begin{array}{l} -\frac{\mathcal{I}}{S}\mathcal{R}(\boldsymbol{\lambda})^S(\mathcal{I}\mathbf{v}_S)_m + \hat{b} \\ + K_1\mathcal{I}\mathcal{R}(\boldsymbol{\lambda})H^{-1}({}^c\hat{\mathbf{p}})(h_{\boldsymbol{\lambda}}({}^c\hat{\mathbf{p}}) - y_m) \end{array} \\ \dot{\hat{b}} & = K_2\mathcal{I}\mathcal{R}(\boldsymbol{\lambda})H^{-1}({}^c\hat{\mathbf{p}})(h_{\boldsymbol{\lambda}}({}^c\hat{\mathbf{p}}) - y_m), \end{cases} \quad (20)$$

where $\hat{\mathbf{p}}$ is the relative position estimate, \hat{b} is the bias estimate, and K_1 and K_2 are gains to be computed so as to meet adequate stability and performance criteria. The estimator structure is depicted in figure 3. The input, state and output vectors are three dimensional. Clearly, this is an LPV system.

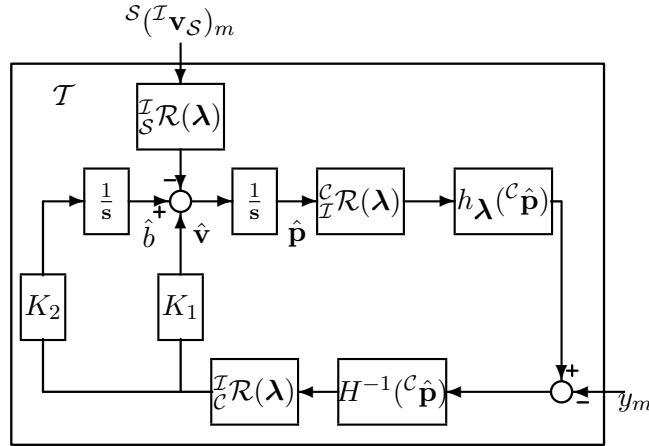


Figure 3: Nonlinear tracker structure.

We now address the problems of regional stability and performance of the filter proposed, referred to as \mathbf{P}_1 and \mathbf{P}_2 respectively, below.

\mathbf{P}_1 Regional Stability - Consider the design model and the estimator structure introduced before. Further assume that $w_v = w_y = 0$. Given an envisioned mission scenario defined by \mathcal{P}_c , find a number $\alpha > 0$ and observer parameters such that the estimates $\hat{\mathbf{p}}$ of \mathbf{p} and $\hat{\mathbf{v}}$ of \mathbf{v} verify the relationships

- a) ${}^c\hat{\mathbf{p}} \in \hat{\mathcal{P}}_c$ for $t > 0$,
- b) $\|\hat{\mathbf{p}} - \mathbf{p}\| + \|\hat{\mathbf{v}} - \mathbf{v}\| \rightarrow 0$ as $t \rightarrow 0$

whenever

$$\|[(\hat{\mathbf{p}}(0) - \mathbf{p}(0))^T, (\hat{\mathbf{b}}(0) - \mathbf{b}(0))^T]^T\|_\infty < \alpha.$$

The next theorem gives conditions under which \mathbf{P}_1 has a solution. The proof is omitted. See theorem 4.3 in (Kaminer *et al.*, 2001) for a similar result.

Theorem 4.2 Consider a mission scenario where the orientation and position variables are constrained by (14) and (15) respectively, and let $\hat{\mathcal{P}}_c$ be given. Let $\alpha < \min(\bar{x} - \underline{x} + dx, \bar{y} - \underline{y} + dy, \bar{z} - \underline{z} + dz)$ be a positive number and define $r_z = \frac{\bar{z} - \underline{z} + dz}{z} < 1$. Further let

$$F := \begin{bmatrix} 0 & I \\ 0 & 0 \end{bmatrix} \quad (21)$$

and $C = [I \ 0]$. Suppose there exists a matrix $P = P^T \in \mathcal{R}^{6 \times 6}$ such that

$$P > 0, \quad (22)$$

$$F^T P + P F + \begin{bmatrix} -2(1 - r_z)^2 I & 0 \\ 0 & 0 \end{bmatrix} < 0, \quad (23)$$

$$P - \max \left(\begin{array}{c} \frac{1}{(\bar{x} - \underline{x} + dx)^2}, \\ \frac{1}{(\bar{y} - \underline{y} + dy)^2}, \\ \frac{1}{(\bar{z} - \underline{z} + dz)^2} \end{array} \right) C^T C > 0, \quad (24)$$

$$\frac{I}{\alpha^2} - P > 0, \quad (25)$$

Then the filter with realization (20) and parameters $K = [K_1^T \ K_2^T]^T = -P^{-1}(1 - r_z)C^T$ solves filtering problem \mathbf{P}_1 .

We now address the more complex problem of filter performance in the presence of sensor noise. Notice how filter performance is captured in terms of a bound on the induced norm of a suitably defined operator.

\mathbf{P}_2 Regional Stability and Performance -

Consider a mission scenario defined by \mathcal{P}_c and $\hat{\mathcal{P}}_c$ in (16). Consider also the design model (13), with $\mathbf{w} = [\mathbf{w}_y^T \ \mathbf{w}_v^T]^T \in L_2$ and $\|\mathbf{w}\|_2 < 1$. Given positive numbers $\gamma > 0$ and $\alpha > 0$ find (if possible) the observer parameters such that

- a) $\|T_{ew}\|_{2,\infty} < \gamma$, where $\mathbf{e} = [(\hat{\mathbf{p}} - \mathbf{p})^T (\hat{\mathbf{b}} - \mathbf{b})^T]^T$ and $T_{ew} : \mathbf{w} \rightarrow \mathbf{e}$;

- b) ${}^c\hat{\mathbf{p}} \in \hat{\mathcal{P}}_c$ for $t > 0$;
- c) $e(t) \rightarrow 0$ as $t \rightarrow \infty$ when $\mathbf{w} = 0$ and $\|[(\hat{\mathbf{p}}(0) - \mathbf{p}(0))^T, (\hat{\mathbf{b}}(0) - \mathbf{b}(0))^T]^T\|_\infty < \alpha$

The next theorem gives conditions under which \mathbf{P}_2 has a solution.

Theorem 4.3 Consider a mission scenario where the orientation and position variables are constrained by (14) and (15) respectively, and let $\hat{\mathcal{P}}_c$ be given. Let $\alpha < \min(\bar{x} - \underline{x} + dx, \bar{y} - \underline{y} + dy, \bar{z} - \underline{z} + dz)$ be a positive number and define $r_z = \frac{\bar{z} - \underline{z} + dz}{\underline{z}} < 1$. Let

$$\begin{aligned} \epsilon &= \min_{\hat{\mathbf{p}}_c \in \hat{\mathcal{P}}_c} \lambda_{\min}(H^{-1}({}^c\hat{\mathbf{p}})H^{-T}({}^c\hat{\mathbf{p}})) \\ &= \min_{\hat{\mathbf{p}}_c \in \hat{\mathcal{P}}_c} \lambda_{\max}(H({}^c\hat{\mathbf{p}})H^T({}^c\hat{\mathbf{p}})) \end{aligned} \quad (26)$$

and given γ , suppose there exists a matrix $P = P^T \in \mathcal{R}^{6 \times 6}$ such that

$$P > 0, \quad (27)$$

$$\left[\begin{array}{c|c} F^T P + P F + \begin{bmatrix} \frac{1}{\gamma^2} & 0 \\ -(1-r_z)^2(2-\epsilon)I & 0 \\ 0 & 0 \end{bmatrix} & P F \\ \hline F^T P & -I \end{array} \right] < 0, \quad (28)$$

$$P - 4 \max \left(\begin{array}{c} \frac{1}{(\bar{x} - \underline{x} + dx)^2}, \\ \frac{1}{(\bar{y} - \underline{y} + dy)^2}, \\ \frac{1}{(\bar{z} - \underline{z} + dz)^2} \end{array} \right) C^T C > 0, \quad (29)$$

$$\frac{I}{\alpha^2} - P > 0. \quad (30)$$

Then, the filter with realization (20) and parameters $K = [K_1^T \ K_2^T]^T = -P^{-1}(1 - r_z)C^T$ solves problem \mathbf{P}_2 if $\|[(\hat{\mathbf{p}}(0) - \mathbf{p}(0))^T, (\hat{\mathbf{b}}(0) - \mathbf{b}(0))^T]^T\|_\infty < \alpha$.

Theorems 4.2 and 4.3 provide adequate tools for the design and analysis of the proposed estimator with complementary filtering properties.

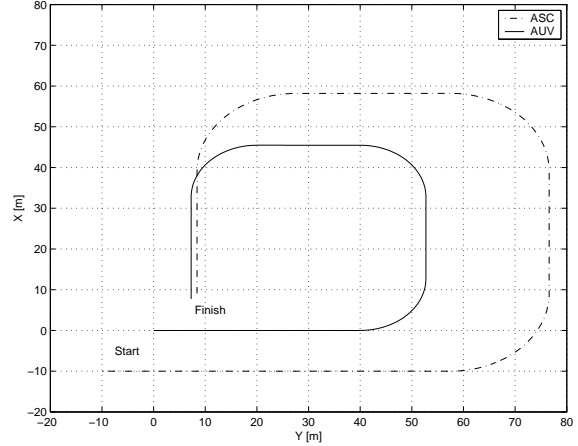


Figure 4: ASC and AUV inertial coordinates in the horizontal plane.

5 Simulation results

This section summarizes the design phase and analyzes briefly the performance of a nonlinear tracker with the structure proposed in (20) for a simulated mission scenario that requires the concerted operation of the AUV and the ASC.

The nominal trajectories performed by the ASC and the AUV are square shaped in the horizontal plane, with constant nominal velocities ${}^S(\mathcal{I}\mathbf{v}_S) = [1.5 \ 0 \ 0]^T$ m/s and ${}^U(\mathcal{I}\mathbf{v}_U) = [1.0 \ 0 \ 0]^T$ m/s, respectively. The ASC remains at the sea surface (${}^I z_s = 0$ m) and the AUV starts the mission at a depth of ${}^I z_u = 30$ m. From time $t = 60$ s until $t = 80$ s the AUV changes its depth with a constant vertical velocity of ${}^I \dot{z}_u = 0.25$ m/s.

The envisioned missions are naturally constrained by the ability of the video camera installed on board the ASC to detect artificial features on the AUV. This impacted on the choice of the parameters for the compact sets \mathcal{P}_c and $\hat{\mathcal{P}}_c$, as shown in table 1. The value of γ in Theorem 4.3 has a lower bound of $\gamma^2 > 55.8$, which is a lower bound on the induced norm $\|T_{ew}\|_{(2,i)}$.

From the LMIs introduced in theorems 4.2 and 4.3 and from the aforementioned parameters, the value for the estimator gains are $K_1 = 0.74 I_{3 \times 3}$ and $K_2 = 0.30 I_{3 \times 3}$, respectively.

In the first experiment, additive gaussian noise with zero mean and a standard deviation of 0.1 m

	Parameter	Value
Λ_c	ϕ_{max}	5°
	θ_{max}	5°
\mathcal{P}_c	$\underline{x} = \underline{y}$	-20 m
	$\bar{x} = \bar{y}$	20 m
	\underline{z}	20 m
	\bar{z}	38 m
$\hat{\mathcal{P}}_c$	dx	0.1 m
	dy	0.1 m
	dz	0.1 m
Theorems 4.2 and 4.3	α	18.1 m
	r_z	0.905 m
Theorem 4.3	ϵ	0.0132

Table 1: Nonlinear tracker design parameters.

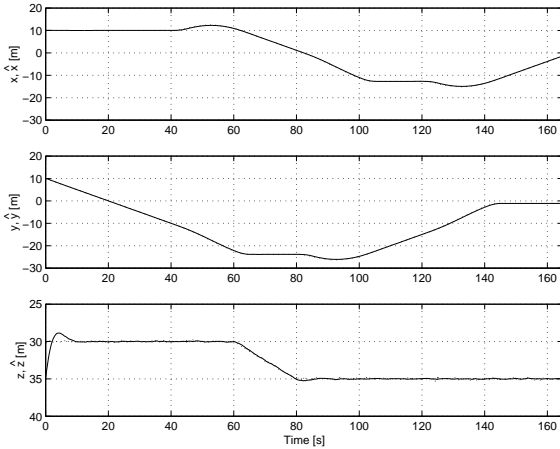


Figure 5: Relative position coordinates \mathbf{p} (dashed) and estimates $\hat{\mathbf{p}} = [\hat{x}\ \hat{y}\ \hat{z}]^T$.

for the depth sensor was considered. The relative z coordinate was initialized at 35 m when the nominal value was 30 m . The results for the relative position \mathbf{p} are depicted in figure 5, which shows very small estimation errors.

A stronger impact of depth sensor noise on the AUV vertical velocity estimate can be observed in figure 6, due to the structure of the estimator chosen. However, the vertical velocity changes are accurately estimated. Finally, the coordinates on the camera plane, after compensation for the focal length frame and without taking into consideration the resolution of the sensing system, are depicted in figure 7 (continuous line).

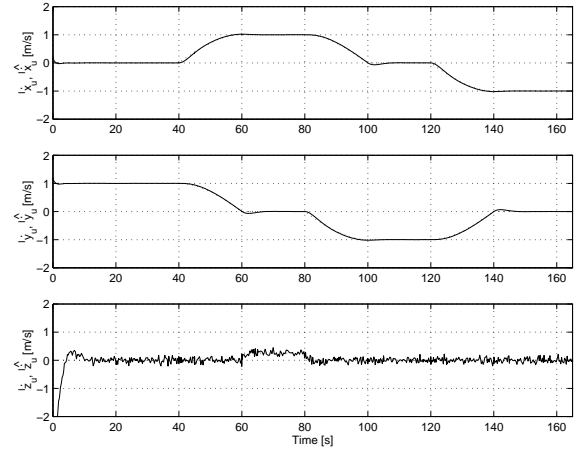


Figure 6: AUV velocity in the inertial frame $\{I\}$ ${}^I\mathbf{v}_U = [{}^I\dot{x}_u\ {}^I\dot{y}_u\ {}^I\dot{z}_u]^T$ (dashed) and respective estimates ${}^I\hat{\dot{x}}_u$, ${}^I\hat{\dot{y}}_u$ and ${}^I\hat{\dot{z}}_u$.

A second experiment was conducted to evaluate the overall performance of the tracker in the presence of a more realistic vision sensor. To that purpose, a resolution grid was set so that a 1 m displacement at a distance of 40 m , in the plane parallel to the camera, would correspond to one pixel. Moreover, an installation error on the camera, corresponding to a rotation on roll, pitch, and yaw angles of 0.1 rad and a misplacement of 0.1 m in all axes was set. The camera plane coordinates are also depicted in figure 7 (dashed line). The impact of such disturbances on the tracking system can be observed in figure 8. Notice that even though the estimates on the relative position becomes biased the tracker exhibits stable characteristics.

6 Conclusions

A nonlinear vision based tracking system was developed to provide estimates of the position and velocity of an Autonomous Underwater Vehicle (AUV) relative to an Autonomous Surface Craft (ASC). Future work will address the problem of tracker stability and performance in the presence of out of frame events that arise when the camera loses temporarily the target due to vehicle rolling

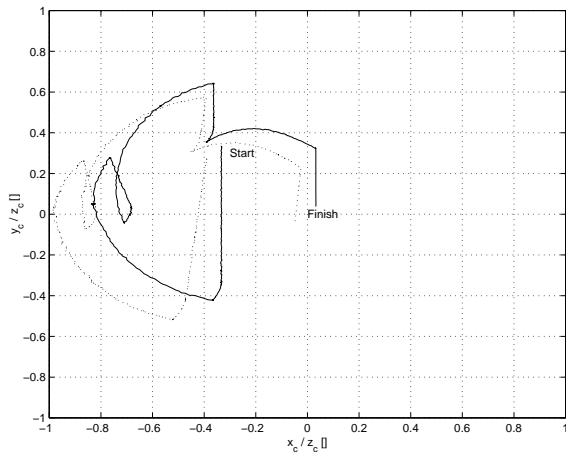


Figure 7: Camera plane coordinates after compensation for the simulated camera parameters. Exact knowledge of the camera position and orientation in the first experiment (continuous line) and misplaced and misdirected (dashed line).

and pitching.

Acknowledgements Research supported in part by the European Community under the research network FREESUB and by the Portuguese FCT agency under project MAROV of the PRAXIS XXI Programme.

References

- ASIMOV (1998-1999). *Advanced System Integration for Managing the Coordinated Operation of Robotic Ocean Vehicles - ASIMOV*. Vol. 1-2. Technical Reports. ISR-IST, Lisbon, Portugal.
- Becker, G. and A. Packard (1994). Robust performance of linear, parametrically varying systems using parametrically dependent linear, dynamic feedback. *Systems and Control Letters* **23**, 205–215.
- Boyd, S., L. El Ghaoui, E. Feron and B. Balakrishnan (1994). *Linear Matrix Inequalities in Systems and Control Theory*. SIAM Studies in Applied Mathematics. Philadelphia.
- Britting, K. (1971). *Inertial Navigation System Analysis*. Wiley-Interscience.
- Horn, B. (1985). *Robot Vision*. MIT Press. Cambridge, MA.

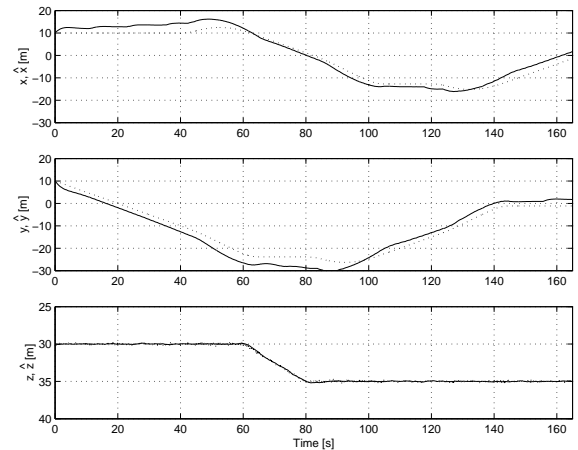


Figure 8: Relative position coordinates \mathbf{p} (dashed) and estimates \hat{x} , \hat{y} and \hat{z} .

IEEE (2000). Ieee control systems magazine, special issue on autonomous unmanned vehicles.

Instrumentation, ORCA (1999). *The GIB System*. Vol. 1. User Manual. Brest, France.

Kaminer, I., W. Kang, O. Yakimenko and A. Pascoal (2001). Application of nonlinear filtering to navigation systems design using passive sensors. *IEEE Electronics and Aerospace Systems* **37**(1), 158–172.

Oliveira, P. (2001). *Periodic and Nonlinear Estimators with Applications to the Navigation of Ocean Vehicles*. PhD Thesis, Instituto Superior Técnico. ISR-IST, Lisbon, Portugal. In English.

Pascoal, A., P. Oliveira, C. Silvestre and et al (2000). Robotic ocean vehicles for marine science applications: the european asimov project. *MTS/IEEE Oceans 2000 Conference*.

Rizzi, A. and D. Koditscheck (1996). An active visual estimator for dextrous manipulation. *IEEE Transactions on Robotics and Automation* **12**(5), 697–713.

Scherer, C. (2000). *Linear Matrix Inequalities in Control*. Class notes.

Vidyasagar, M. (1985). *Control System Synthesis: a Factorization Approach*. MIT Press.